ACS POLYMERS Au
AN OPEN ACCESS JOURNAL OF THE AMERICAN CHEMICAL SOCIETY

pubs.acs.org/polymerau

Article

Lewis Adduct-Induced Phase Transitions in Polymer/Solvent Mixtures

Tylene Hilaire, Yifan Xu, Wenwen Mei, Robert A. Riggleman, and Robert J. Hickey*

Cite This: *ACS Polym. Au* 2022, 2, 35–41

Read Online

ACCESS | Metrics & More | Article Recommendations | Supporting Information

ABSTRACT: Functionalization-induced phase transitions in polymer systems in which a postpolymerization reaction drives polymers to organize into colloidal aggregates are a versatile method to create nanoscale structures with applications related to biomedicine and nanoreactors. Current functionalization methods to stimulate polymer self-assembly are based on covalent bond formation. Therefore, there is a need to explore alternative reactions that result in noncovalent bond formation. Here, we demonstrate that when the Lewis acid, tris(pentafluorophenyl) borane (BCF), is added to a solution containing poly(4-diphenylphosphino styrene) (PDPPS), the system will either macrophase-separate or form micelles if PDPPS is a homopolymer or a block in a copolymer, respectively. The Lewis adduct-induced phase transition is hypothesized to result from the favorable interaction between the PDPPS and BCF, which results in a negative interaction parameter (χ). A modified Flory–Huggins model was used to determine the predicted phase behavior for a ternary system composed of a polymer, a solvent, and a small molecule. The model indicates that there is a demixing region (i.e., macrophase separation) when the polymer and small molecule have favorable interactions (e.g., $\chi < 0$) and that the phase separation region coincides well with the experimentally determined two-phase region for mixtures containing PDPPS, BCF, and toluene. The work presented here highlights that Lewis adduct-induced phase separation is a new approach to functionalization-induced self-assembly (FISA) and that ternary mixtures will undergo phase separation if two of the components exhibit a sufficiently negative χ.

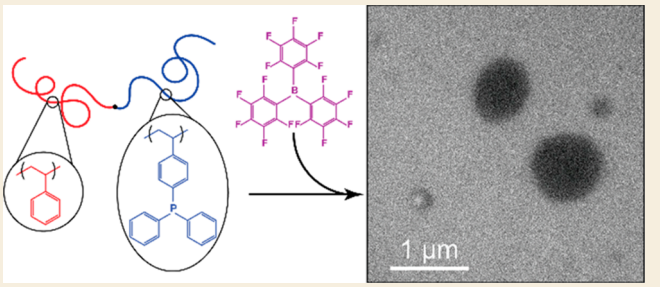

KEYWORDS: *Functionalization, Induced Phase Transitions, Self-Assembly, Lewis Adduct, Flory–Huggins, Negative χ*

INTRODUCTION

Driving morphological transitions in polymer systems via local molecular changes using chemical reactions opens exciting opportunities to create stimuli-responsive materials.[1] The process of using chemical reactions such as functionalization,[2−4] deprotection,[5] conjugation,[6] chain-scission,[7] or polymerization[8−10] to induce changes in a system falls under the broad area of the reaction-induced phase transition (RIPT).[11] Functionalization-induced self-assembly (FISA), in particular, is a promising approach in creating colloidal nanostructures with access to various aggregate morphologies with applications in biomedical imaging,[12−14] drug delivery,[7] and catalysis.[15] The use of FISA in AB diblock copolymer systems uses postpolymerization chemical modification methods to convert one polymer block that initially exhibits favorable polymer–solvent interactions to one that will separate from the solvent forming nanoscale aggregates due to unfavorable interactions. Recent advances in FISA include Pd-catalyzed Suzuki–Miyaura cross-coupling,[3] azo-coupling,[2] and thiol-epoxide ring-opening reactions.[4] In all the FISA examples, the size of the micelles after the reaction is ultimately dictated by the molecular weight of the reactive polymer block, but intermediate sizes are possible by controlling the extent of functionalization. Beyond the reported FISA reactions, there are numerous postpolymerization functionalization strategies to promote block polymer self-assembly in a controlled manner and to tailor desired chemistries.[16]

Previous FISA techniques used nonreversible covalent bonds to create self-assembled nanostructures, and once the nanostructures are formed, disassembly of the aggregates is difficult due to the formation of strong covalent bonds. To expand the versatility of FISA in block copolymer systems to create nanostructures that are able to transition between two different morphologies, reversible and dynamic bonding triggered via external stimuli is necessary.[1] Common reversible and dynamic bonds encompass a broad spectrum of bond strengths ranging from weak $\pi-\pi$ stacking and hydrogen bonding to strong alkoxyamine cross-links and Diels–Alder chemistry.[17−20] Although dynamic chemical bonds are ideal for

Received: August 15, 2021
Revised: October 29, 2021
Accepted: November 1, 2021
Published: November 17, 2021

https://doi.org/10.1021/acspolymersau.1c00024
ACS Polym. Au 2022, 2, 35–41

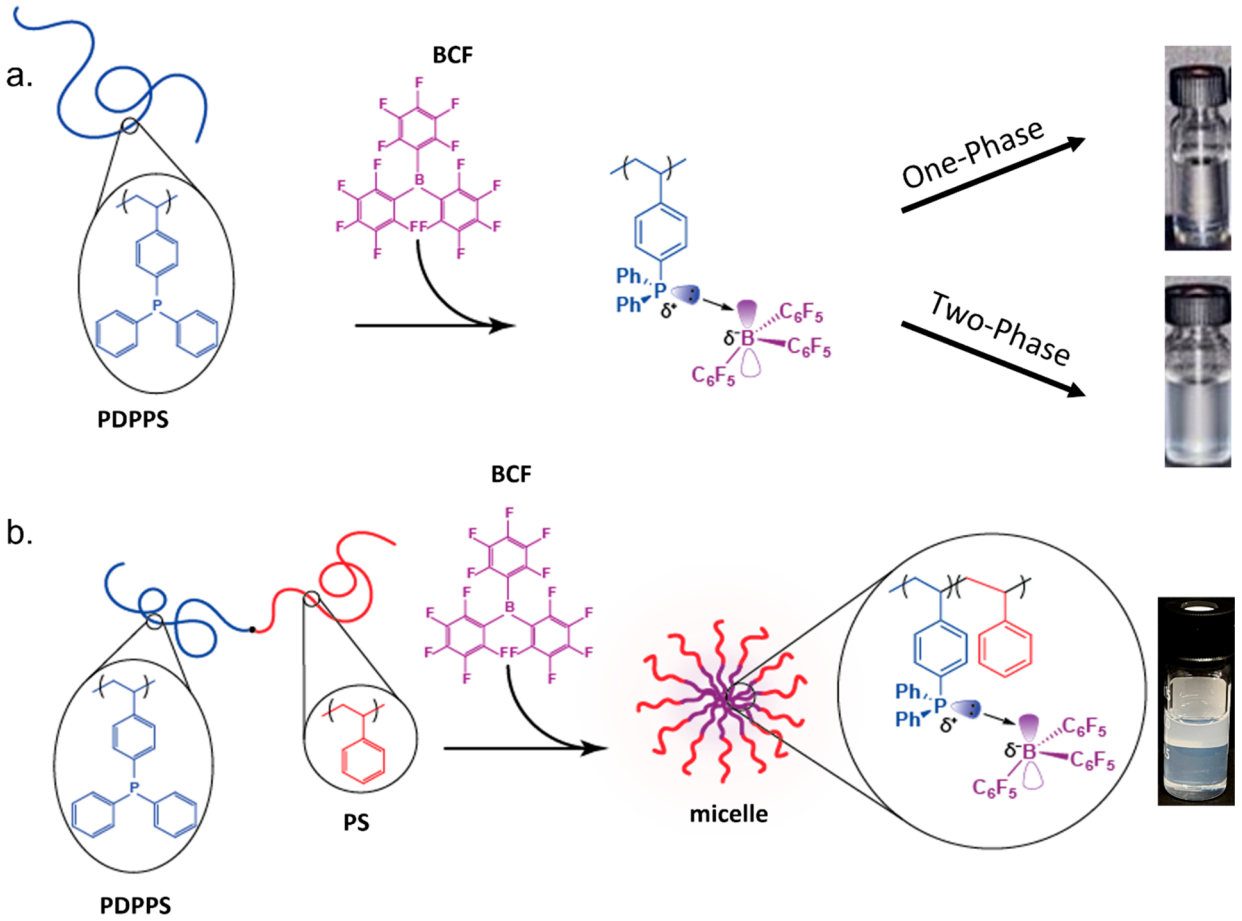

Figure 1. Schematic representation of Lewis adduct-induced phase separation in PDPPS homopolymer and diblock copolymer systems. When BCF is added to a polymer solution containing PDPPS that exceeds a B/P molar ratio threshold value, the system will either (a) macrophase-separate forming a two-phase mixture or (b) form nanoscale colloidal aggregates.

responsive polymer networks that are recyclable and healable as well as exhibiting tunable mechanical properties (e.g., transitioning between stiff and soft),[20] the chemical bonds either do not influence or have minimal impact on the polymer chemical interaction with the environment, preventing induced changes in the nanostructure as a result of chemical bonding. Therefore, it is pertinent to explore alternative reversible and dynamic bonding motifs that lead to changes in the polymer chemical interaction that will induce nanoscale transitions between different phases.

A class of reversible and dynamic noncovalent bonds that involve donor−acceptor interactions are Lewis pairs, in which the Lewis acid (LA) accepts an electron lone pair from the Lewis base (LB) to form a dative bond.[21,22] A distinctive feature of Lewis adducts is that the binding energy of the dative bond is tunable by electronic and steric modifications of the LA or the LB.[21,23] In a classic Lewis adduct involving boron trihydride and ammonia, the bond dissociation energy is estimated as 31 kcal/mol, which is approximately a third of the bond dissociation energy needed for a carbon−carbon single bond.[24] Therefore, it is possible to tailor specific bond energies in Lewis adduct macromolecular systems to tune the properties of materials for specific applications such as sensors, gas storage, or catalysis.[25] The dynamic adduct has been recently used to synthesize reversible polymer networks that are self-healing; however, a fundamental understanding related to the influence of the formation of Lewis adducts on polymer self-assembly has yet to be determined.[18,26] For example, work from Yan and co-workers showed that the addition of CO_2 to a solution containing two different diblock copolymers where both had poly(styrene) (PS) as one block and either a polyLA (i.e., poly(4-styryl-di(pentafluorophenyl)borane)) or a polyLB (i.e., poly(4-styryldimesitylphosphine)) induced micellization,[27] but the underlying self-assembly process is still unknown. Incorporating Lewis adduct chemistry to induce self-assembly is an effective method to synthesize tailorable and responsive nanostructures with biomedical and catalysis applications.

In an effort to determine the impact of Lewis adduct formation on solution polymer self-assembly, we uncovered for the first time that Lewis adduct formation drives macrophase and nanoscale phase transitions when a small molecule Lewis acid is added to either a poly(LB) homopolymer or diblock copolymer while in solution. Specifically, when the Lewis acid tris(pentafluorophenyl) borane (BCF) is added to a solution containing a poly(LB) such as poly(4-diphenylphosphino styrene) (PDPPS), the system will either macrophase-separate or form micelles if PDPPS is a homopolymer or a block in a copolymer, respectively (Figure 1). ^{31}P nuclear magnetic resonance (NMR) was used to confirm that indeed the Lewis adduct is formed, but the bond is weak as quantified by measuring the dissociation constant (K_d). Although the K_d value indicates that the B/P bond is weak, the adduct formation has a major impact on the self-assembly of the

https://doi.org/10.1021/acspolymersau.1c00024
ACS Polym. Au 2022, 2, 35−41

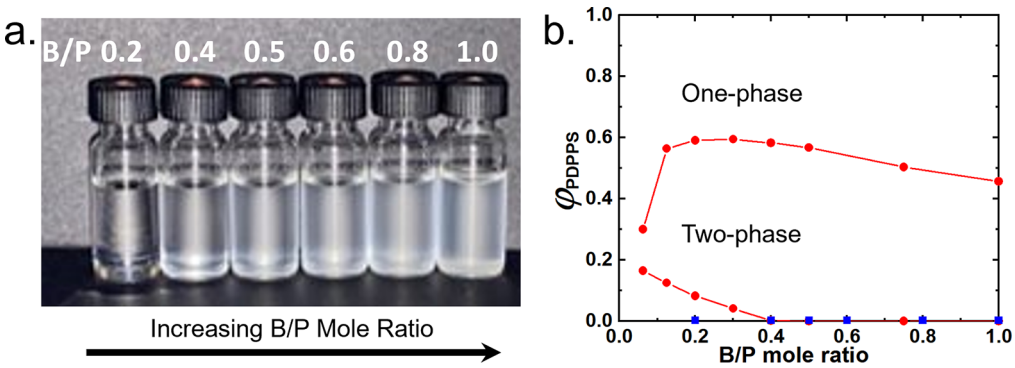

Figure 2. Determining the ternary phase behavior for mixtures containing PDPPS (M_n = 3.9 kg/mol), BCF, and toluene. (a) Visual assessment of one-phase and two-phase mixtures with an increasing B/P mole ratio. One-phase solutions are clear and colorless, while two-phase samples are cloudy, indicating that the polymer is phase-separated from toluene. (b) Predicted ternary phase behavior with respect to B/P mole ratio using a modified Flory–Huggins model, in which two components have favorable interactions. The red points connected by red lines are equilibrium coexistence concentrations from a fully fluctuating simulation of the model, and the blue points are experimentally determined data points shown in Figure 2a.

polymers. The Lewis adduct-induced phase transition is hypothesized to result from the favorable interaction between the PDPPS and BCF, which results in a negative interaction parameter (χ). A modified Flory–Huggins model was used to determine the predicted phase behavior for a ternary system composed of a polymer, a solvent, and a small molecule. The model indicates that there is a demixing region (i.e., macrophase separation) when the polymer and small molecule have favorable interactions (e.g., $\chi < 0$) and that the phase separation region coincides well with the experimentally determined two-phase region for mixtures containing PDPPS, BCF, and toluene. The work presented here highlights that Lewis adduct-induced phase separation is a new approach to FISA and that ternary mixtures will undergo phase separation if two of the components exhibit negative χ.

RESULTS AND DISCUSSION

Two poly(LB)s containing PDPPS were synthesized with controlled molecular weight and diblock copolymer composition to establish how the formation of a Lewis adduct drives phase transitions (Figure 1). Two different synthetic methods, living anionic polymerization and reversible addition–fragmentation chain-transfer (RAFT) polymerization, were used to synthesize the PDPPS homopolymer and the diblock copolymer, respectively. The homopolymer, synthesized using a modified living anionic polymerization procedure,[28] exhibited a number-average molecular weight (M_n) and a dispersity ($Đ$) of 3.9 kg/mol and 1.13, respectively. The PDPPS–PS diblock copolymer was synthesized using sequential RAFT polymerization and had an M_n, a $Đ$, and a PDPPS volume fraction (f_{PDPPS}) of 21.9 kg/mol, 1.19, and 0.17, respectively. The density of PS at 140 °C (e.g., 0.969 g/cm^3) was used for both PDPPS and PS blocks to calculate f_{PDPPS}.[29] Sequential RAFT polymerization was utilized to synthesize a diblock copolymer because of the residual PDPPS homopolymer in the PDPPS–PS diblock copolymer sample synthesized using living anionic polymerization. Molecular weight and dispersity were determined using size-exclusion chromatography (SEC) calibrated against PS standards. Synthetic details and characterization results are in the Supporting Information.

First, the influence of Lewis adduct formation on the phase behavior of a ternary mixture containing PDPPS, BCF, and toluene (Tol) were systematically studied by changing the B/P mole ratio (Figure 2a). In a typical experiment, BCF/Tol solutions (2.1, 4.2, 5.25, 6.3, 8.4, and 10.5 mg/mL) corresponding to B/P ratios of 0.2, 0.4, 0.5, 0.6, 0.8, and 1.0 were added to individual PDPPS solutions in toluene (5.5 mg/mL) while stirring and visually assessed to determine one-phase and two-phase regions (Figure 2a). At low B/P mole ratios (B/P < 0.4), the ternary mixtures were clear and colorless, indicating a one-phase mixture. At elevated B/P mole ratios (B/P ≥ 0.4), the mixtures become cloudy, signaling that the samples macrophase-separate (Figure 2a). The phase separation results shown in Figure 2a were unexpected, as both PDPPS and BCF are individually soluble in toluene.

To gain insight into the phase separation behavior for the ternary mixture containing PDPPS, BCF, and Tol, a predicted phase diagram was established using a modified Flory–Huggins model (Figure 2b). Specifically, the free energy of mixing (F) was calculated using

$$F = \varphi_{PDPPS}\log\varphi_{PDPPS} + \varphi_{BCF}\log\varphi_{BCF} + \varphi_{Tol}\log\varphi_{Tol} + \chi_{PDPPS/BCF}\varphi_{PDPPS}\varphi_{BCF} \quad (1)$$

where φ and $\chi_{PDPPS/BCF}$ are the volume fraction of the designated component and the Flory–Huggins interaction parameter between PDPPS and BCF, respectively. Here, it is assumed that interactions between either PDPPS or BCF are neutral with toluene ($\chi_{PDPPS/Tol} = \chi_{BCF/Tol} = 0$), and a molar ratio between PDPPS and BCF is $\varphi_{BCF} = f\varphi_{PDPPS}$, which determines the stoichiometric ratio between the B and P. Here, $\chi_{BCF/Tol}$ is set to 0 to simplify the phase diagram, but arene–perfluoroarene interactions are not insignificant[30] and would result in $\chi_{BCF/Tol} < 0$. Furthermore, the mole balance requires that $\varphi_{Tol} = 1 - \varphi_{PDPPS} - \varphi_{BCF} = 1 - (1 + f)\varphi_{PDPPS}$. Finally, the volumetric degrees of polymerizations (N) used to predict the phase diagram are 38, 3, and 1 for PDPPS, BCF, and toluene, respectively. The volume of toluene was used as the reference volume. We note that while more sophisticated treatments are possible,[31] systems with donor/acceptor interactions such as those present here have been successfully modeled in the past using a simple negative χ parameter.[32]

If $\chi_{PDPPS/BCF}$ is sufficiently negative, an unstable region occurs, in which the PDPPS and BCF adduct will phase separate from toluene. Specifically, when $\chi_{PDPPS/BCF} = -7.5$, the predicted ternary phase diagram is shown in Figure 2b, in

https://doi.org/10.1021/acspolymersau.1c00024
ACS Polym. Au 2022, 2, 35–41

which the φ_{PDPPS} is plotted versus B/P mole ratio and agrees well with the experimentally determined one-phase and two-phase regions at constant φ_{PDPPS} and varying B/P mole ratio. For example, the simulation points in the phase diagram calculated using dynamic simulations[33] suggest that the ternary mixture is one-phase when B/P < 0.2 and that the concentration of polymer in the polymer-rich phase goes through a maximum at B/P ≈ 0.3. In addition to simulating the phase diagram in Figure 2b when $\chi_{PDPPS/Tol} = \chi_{BCF/Tol} = 0$ and $\chi_{PDPPS/BCF} = -7.5$, supplementary simulations were conducted to gain insight into the effect of changing BCF/Tol interactions (e.g., $\chi_{BCF/Tol} \neq 0$). Specifically, the interaction parameter between BCF/Tol was varied from favorable (e.g., $\chi_{BCF/Tol} = -1$) to unfavorable (e.g., $\chi_{BCF/Tol} = 1$), which still resulted in a demixing region for both conditions, but the breadth of the two-phase window increased with unfavorable BCF/Tol interactions (See Figure S8 in the SI). More in-depth studies include experimentally measuring χ or using a more sophisticated approach that models binding of components as a chemical reaction to justify the use of such a strongly negative $\chi_{PDPPS/BCF}$ value.[31]

The formation of the Lewis adduct and the dissociation constant (K_d) between BCF and the P in PDPPS were confirmed and quantified, respectively, using ^{31}P NMR (Figure 3). A series of PDPPS/BCF solutions in toluene with varying

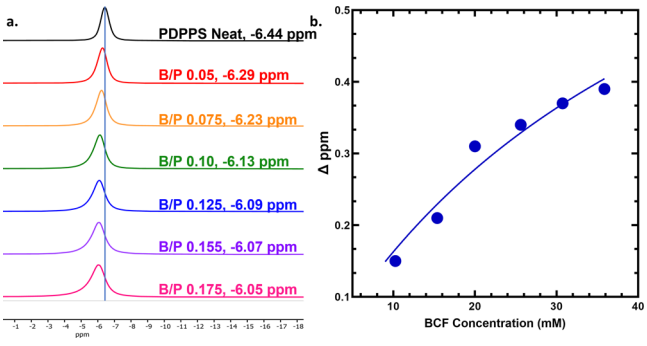

Figure 3. ^{31}P NMR spectra and binding isotherm to determine K_d. (a) ^{31}P NMR spectra for PDPPS/BCF mixtures in toluene at different B/P mole ratios (B/P = 0−0.175). The vertical blue line is to indicate the change in ppm with increasing B/P mole ratio. M_n = 3.9 kg/mol for PDPPS. (b) Binding isotherm for the titration of BCF to PDPPS in toluene. The solid blue line is the fit using a single binding model for the 1:1 stoichiometric reaction between B and P. See the Supporting Information for details.

B/P mole ratios were prepared via titration, and the change in the chemical shift (Δppm, which is the difference in ppm between the neat PDPPS and the PDPPS/BCF mixtures) was recorded. All prepared solutions were in the one-phase region (B/P < 0.4). Figure 3a shows a downfield shift in the ^{31}P NMR peak associated with the P nuclei of the PDPPS and is indicative of the deshielding of the phosphorus nuclei when the P and B form an adduct. The plot in Figure 3b shows the change in Δppm with respect to the BCF concentration for PDPPS. Additional ^{19}F NMR titration experiments were conducted for the small molecule triphenyl phosphine (TPP), which is a small molecule analogue of PDPPS, and BCF (see Supporting Information). The binding between PDPPS and BCF is expected, as previously reported studies show that the small molecule mixtures (TPP/BCF) do form adducts.[34,35] Fitting the graph in Figure 3b with a single binding model for the 1:1 stoichiometric reaction between B and P allows for the determination of K_d.[36] The PDPPS/BCF adduct exhibits a $K_d = 4.8 \times 10^{-2}$ M, while the TPP/BCF complex exhibits K_d values of 2.8×10^{-2} and 2.2×10^{-2} M by tracking the ppm change in the ^{19}F NMR spectra using the *ortho* and *meta* positions of BCF (see Supporting Information). K_d values for both PDPPS/BCF and TPP/BCF are within the same order of magnitude, indicating that the binding between P and B in both systems is similar. The reported K_d values indicate that the binding between P and B for the Lewis adducts explored is weak but is stronger than the measured K_d for the BCF and tris(2,4,6-trimethylphenyl)phosphine adduct, which is reported to be on average 2 M.[37] The difference between K_d values is predicted to be a result of the increased bulkiness of tris(2,4,6-trimethylphenyl)phosphine and the stronger arene−perfluoroarene intermolecular interactions with BCF and PDPPS.[30] Although the binding between PDPPS/BCF is considered weak, it has a drastic effect on the phase behavior of the ternary system. It is important to note that the BCF was used as received and contains bound water, as confirmed with ^{19}F NMR and is consistent with a previous report.[38] Therefore, the BCF molecules with bound water will have to either displace the water during Lewis adduct formation or $[BCF{-}OH]{-}[HPPh_3]^+$ forms, which will still lead to phase separation.

FISA to create nanoscale colloidal aggregates using Lewis adduct formation was demonstrated with a PDPPS−PS diblock copolymer (Figure 4). As shown in Figure 2, the PDPPS homopolymer will macrophase-separate when the B/P mole ratio is greater than or equal to 0.4. In colloidal AB diblock copolymer systems, nanoscale colloidal structures adopt a core−corona structure, in which one polymer block forms a shell swollen with solvent around the core, stabilizing the aggregate, while the incompatible block forms the core.[39] For aqueous systems, a solvent switch method is generally used, in which water is slowly added to an amphiphilic diblock copolymer solution containing a water miscible organic solvent such as tetrahydrofuran, driving the hydrophobic block to aggregate as the water content is increased.[39] Here, the self-assembly process for PDPPS−PS diblock copolymers with the addition of BCF is related to standard solvent switch methods, but instead of gradually varying solvent composition, the B/P mole ratio is tuned. Therefore, to induce nanoscale self-assembly, a BCF/Tol solution is slowly added to a PDPPS−PS/Tol solution at the rate of 0.20 mL/30 s at room temperature while stirring. The BCF concentration in the BCF/Tol solution is adjusted to achieve the desired B/P mole ratio.

The dynamic light scattering (DLS) results and transmission electron microscopy (TEM) images confirm the formation of nanoscale aggregates when BCF is added to a PDPPS−PS/Tol solution (Figure 4). When B/P = 0, the DLS results indicate that the PDPPS−PS diblock copolymer exhibits a hydrodynamic diameter (d_H) of 8.3 nm, which is from the single diblock copolymer chain. When the B/P mole ratio is increased to 0.6, a second peak is seen at d_H = 22.1 nm, which is attributed to the formation of micelles. In addition to the second peak that forms when B/P = 0.6, the peak associated with the free PDPPS−PS diblock copolymer is also present. When the B/P mole ratio is increased further to 0.8 and 1.0, a much larger peak is seen that corresponds to aggregates that are on average 785 nm. The TEM image in Figure 4b confirms that the colloidal aggregates that form are

https://doi.org/10.1021/acspolymersau.1c00024
ACS Polym. Au 2022, 2, 35−41

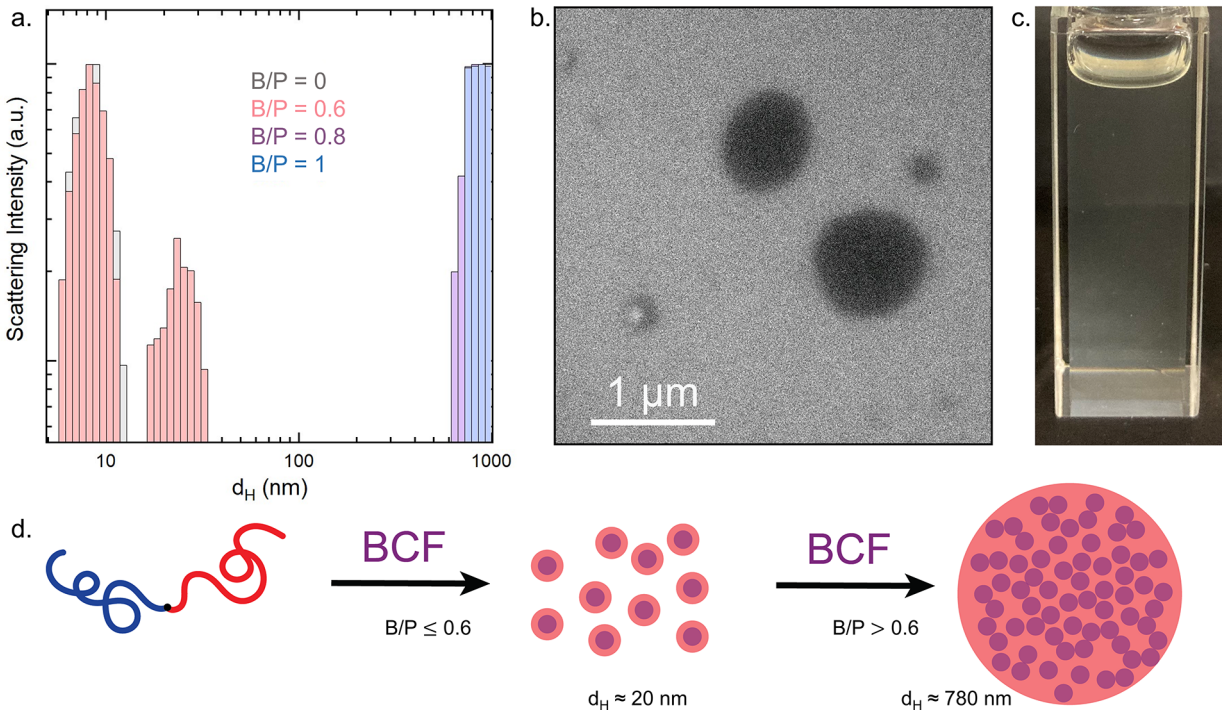

Figure 4. Characterization of nanoscale colloidal aggregates that form using Lewis adduct-induced self-assembly. (a) Hydrodynamic diameter size distribution of PDPPS−PS/BCF mixtures measured by DLS at 90°. (b) TEM image of a PDPPS−PS/BCF mixture when B/P = 0.8. The sample was prepared by drop-casting the solution onto a TEM grid. (c) Photograph of a PDPPS−PS/BCF solution when B/P = 0.8. (d) Scheme depicting the proposed two-step nanoscale self-assembly process with an increasing B/P mole ratio.

on the order of 1 μm. The photograph in Figure 4c is for a sample with B/P = 0.8 and shows that although the colloidal aggregates that form are large, the sample is colloidally stable as compared to the photograph shown in Figure 2a for the PDPPS homopolymer sample at the same B/P mole ratio.

The DLS results in Figure 4a indicate that there is a two-step self-assembly process with an increasing B/P mole ratio. The first step involves forming isolated micelles, whereas the second step is predicted to correspond to the aggregation of the micelles. The schematic shown in Figure 4d shows the progression from a PDPPS/toluene solution containing single diblock copolymer chains when B/P = 0, to isolated micelles when B/P ≤ 0.6, and finally to micellar aggregates when B/P > 0.6. Although the predicted isolated micelle structure is expected to consist of a core containing the PDPPS/BCF Lewis adduct and the corona consisting of the PS block swollen with toluene, additional experiments are necessary to confirm the proposed structure. The large aggregates that form when B/P > 0.6 are hypothesized to be micellar aggregates, because it is not possible for the core size of a single micelle to be greater than a few tens of nanometers when the PDPPS block molecular weight is M_n = 3.6 kg/mol. The reason for the formation of large micellar aggregates when B/P > 0.6 is still under investigation.

Adding a stronger Lewis base such as triethylamine (TEA) to a PDPPS−PS/BCF mixture containing colloidal aggregates will reverse the micellization process (Figure 5). As shown in Figure 5, when a mole ratio of TEA/BCF = 1:1 is added to a PDPPS−PS/BCF mixture containing large micelles (e.g., $d_H \approx$ 780 nm) when B/P = 0.8, the micelle size decreases. Although there are still small micelles left, free PDPPS−PS chains are present. We hypothesize that the addition of TEA will preferentially bind to the BCF, reversing the Lewis adduct-induced self-assembly between PDPPS−PS/BCF. We are currently exploring methods to completely reverse the micellization.

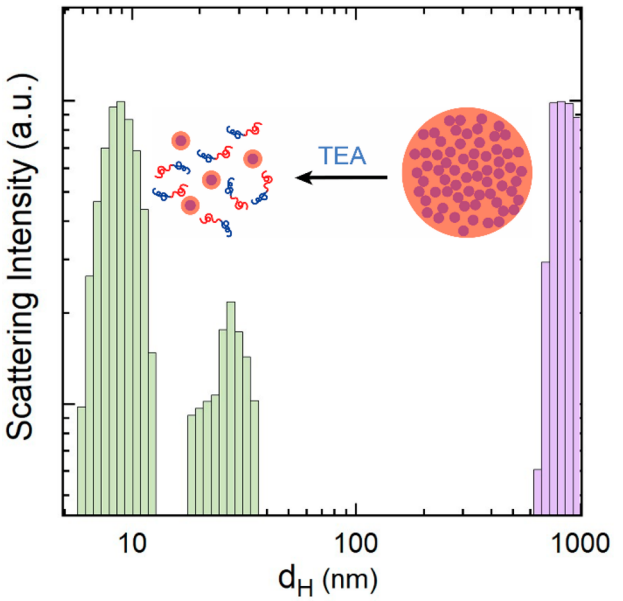

Figure 5. DLS histogram showing a decrease in the hydrodynamic diameter of colloidal aggregates formed when triethylamine (TEA) is added to a PDPPS−PS mixture at B/P = 0.8. When a mole ratio of TEA/BCF = 1:1, the resulting mixture contains both isolated micelles and single PDPPS−PS chains.

https://doi.org/10.1021/acspolymersau.1c00024
ACS Polym. Au 2022, 2, 35−41

CONCLUSIONS

Here, we demonstrate a new FISA method for creating self-assembled nanoscale structures using Lewis adduct formation. We use a modified Flory−Huggins mixing theory to predict the phase behavior of a ternary mixture containing PDPPS, BCF, and toluene, and the results are in accordance with the experimentally determined phase behavior. Flory−Huggins theory indicates that there is a region in phase space in which two components will phase separate when the interaction between the two species is favorable (e.g., $\chi_{PDPPS/BCF} < 0$). The realization that ternary mixtures in which two species exhibit a negative χ value will lead to phase separation under specific conditions has broad implications in different macromolecular systems. The phase separation behavior of the PDPPS homopolymer with the addition of BCF was used to induce micelle formation in a PDPPS−PS diblock system in which the PDPPS/BCF adduct forms the core and the PS block forms the corona. The PDPPS−PS self-assembly progression undergoes a two-step process, in which isolated micelles form first and then aggregate, resulting in large colloidal aggregates that are still colloidally stable, as opposed to the neat PDPPS homopolymer system that macrophase-separates. Furthermore, the addition of a stronger base such as TEA will reverse the micellization process. The use of Lewis adducts to induce polymer self-assembly opens new ways to create colloidal nanostructures displaying stimuli-responsive properties due to the reversible and dynamic noncovalent bonding afforded by the Lewis acid/base pair.

ASSOCIATED CONTENT

Supporting Information

The Supporting Information is available free of charge at https://pubs.acs.org/doi/10.1021/acspolymersau.1c00024.

Experimental details, polymer characterization such as ^{1}H and ^{31}P NMR, and descriptions of binding constant fitting parameters and calculated phase diagram (PDF)

AUTHOR INFORMATION

Corresponding Author

Robert J. Hickey − *Department of Materials Science and Engineering and Materials Research Institute, The Pennsylvania State University, University Park, Pennsylvania 16801, United States;* orcid.org/0000-0001-6808-7411; Email: rjh64@psu.edu

Authors

Tylene Hilaire − *Department of Chemistry, The Pennsylvania State University, University Park, Pennsylvania 16801, United States*

Yifan Xu − *Department of Materials Science and Engineering, The Pennsylvania State University, University Park, Pennsylvania 16801, United States;* orcid.org/0000-0001-8393-4439

Wenwen Mei − *Department of Materials Science and Engineering, The Pennsylvania State University, University Park, Pennsylvania 16801, United States*

Robert A. Riggleman − *Department of Chemical and Biomolecular Engineering, University of Pennsylvania, Philadelphia, Pennsylvania 19104, United States;* orcid.org/0000-0002-5434-4787

Complete contact information is available at: https://pubs.acs.org/10.1021/acspolymersau.1c00024

Notes

The authors declare no competing financial interest.

ACKNOWLEDGMENTS

This work is supported by the Air Force Office of Scientific Research (AFOSR) under the Young Investigator Prize (Award: 18RT0680). We also thank Chang Liu from the Cremer Group at Penn State for his help and advice on dynamic light scattering measurements and Dr. Christy George at the Penn State NMR Facility for assistance conducting NMR measurements and interpreting data.

REFERENCES

(1) Stuart, M. A. C.; Huck, W. T. S.; Genzer, J.; Müller, M.; Ober, C.; Stamm, M.; Sukhorukov, G. B.; Szleifer, I.; Tsukruk, V. V.; Urban, M.; Winnik, F.; Zauscher, S.; Luzinov, I.; Minko, S. Emerging applications of stimuli-responsive polymer materials. *Nat. Mater.* **2010**, *9*, 101−113.

(2) Li, S.; Wang, J.; Shen, J.; Wu, B.; He, Y. Azo Coupling Reaction Induced Macromolecular Self-Assembly in Aqueous Solution. *ACS Macro Lett.* **2018**, *7*, 437−441.

(3) Howe, D. H.; Hart, J. L.; McDaniel, R. M.; Taheri, M. L.; Magenau, A. J. D. Functionalization-Induced Self-Assembly of Block Copolymers for Nanoparticle Synthesis. *ACS Macro Lett.* **2018**, *7*, 1503−1508.

(4) Howe, D. H.; Jenewein, K. J.; Hart, J. L.; Taheri, M. L.; Magenau, A. J. D. Functionalization-induced self-assembly under ambient conditions via thiol-epoxide "click" chemistry. *Polym. Chem.* **2020**, *11*, 298−303.

(5) Qi, W.; Zhang, Y.; Wang, J.; Tao, G.; Wu, L.; Kochovski, Z.; Gao, H.; Chen, G.; Jiang, M. Deprotection-Induced Morphology Transition and Immunoactivation of Glycovesicles: A Strategy of Smart Delivery Polymersomes. *J. Am. Chem. Soc.* **2018**, *140*, 8851−8857.

(6) Chen, L.; Xu, M.; Hu, J.; Yan, Q. Light-Initiated in Situ Self-Assembly (LISA) from Multiple Homopolymers. *Macromolecules* **2017**, *50*, 4276−4280.

(7) Ahmed, F.; Pakunlu, R. I.; Brannan, A.; Bates, F.; Minko, T.; Discher, D. E. Biodegradable polymersomes loaded with both paclitaxel and doxorubicin permeate and shrink tumors, inducing apoptosis in proportion to accumulated drug. *J. Controlled Release* **2006**, *116*, 150−158.

(8) Canning, S. L.; Smith, G. N.; Armes, S. P. A Critical Appraisal of RAFT-Mediated Polymerization-Induced Self-Assembly. *Macromolecules* **2016**, *49*, 1985−2001.

(9) Zofchak, E. S.; LaNasa, J. A.; Mei, W.; Hickey, R. J. Polymerization-Induced Nanostructural Transitions Driven by In Situ Polymer Grafting. *ACS Macro Lett.* **2018**, *7*, 822−827.

(10) Zofchak, E. S.; LaNasa, J. A.; Torres, V. M.; Hickey, R. J. Deciphering the Complex Phase Behavior during Polymerization-Induced Nanostructural Transitions of a Block Polymer/Monomer Blend. *Macromolecules* **2020**, *53*, 835−843.

(11) Lequieu, J.; Magenau, A. J. D. Reaction-induced phase transitions with block copolymers in solution and bulk. *Polym. Chem.* **2021**, *12*, 12−28.

(12) Hickey, R. J.; Haynes, A. S.; Kikkawa, J. M.; Park, S.-J. Controlling the Self-Assembly Structure of Magnetic Nanoparticles and Amphiphilic Block-Copolymers: From Micelles to Vesicles. *J. Am. Chem. Soc.* **2011**, *133*, 1517−1525.

(13) Hickey, R. J.; Koski, J.; Meng, X.; Riggleman, R. A.; Zhang, P.; Park, S.-J. Size-Controlled Self-Assembly of Superparamagnetic Polymersomes. *ACS Nano* **2014**, *8*, 495−502.

(14) Hickey, R. J.; Meng, X.; Zhang, P.; Park, S.-J. Low-Dimensional Nanoparticle Clustering in Polymer Micelles and Their Transverse Relaxivity Rates. *ACS Nano* **2013**, *7*, 5824−5833.

(15) Zhang, J.-T.; Wei, G.; Keller, T. F.; Gallagher, H.; Stötzel, C.; Müller, F. A.; Gottschaldt, M.; Schubert, U. S.; Jandt, K. D. Responsive Hybrid Polymeric/Metallic Nanoparticles for Catalytic Applications. *Macromol. Mater. Eng.* **2010**, *295*, 1049−1057.
(16) Günay, K. A.; Theato, P.; Klok, H.-A. Standing on the shoulders of Hermann Staudinger: Post-polymerization modification from past to present. *J. Polym. Sci., Part A: Polym. Chem.* **2013**, *51*, 1−28.
(17) Van Ruymbeke, E. Preface: Special Issue on Associating Polymers. *J. Rheol.* **2017**, *61*, 1099−1102.
(18) Vidal, F.; Gomezcoello, J.; Lalancette, R. A.; Jäkle, F. Lewis Pairs as Highly Tunable Dynamic Cross-Links in Transient Polymer Networks. *J. Am. Chem. Soc.* **2019**, *141*, 15963−15971.
(19) Jin, K.; Li, L.; Torkelson, J. M. Recyclable Crosslinked Polymer Networks via One-Step Controlled Radical Polymerization. *Adv. Mater.* **2016**, *28*, 6746−6750.
(20) Sun, H.; Kabb, C. P.; Dai, Y.; Hill, M. R.; Ghiviriga, I.; Bapat, A. P.; Sumerlin, B. S. Macromolecular metamorphosis via stimulus-induced transformations of polymer architecture. *Nat. Chem.* **2017**, *9*, 817.
(21) Yolsal, U.; Horton, T. A. R.; Wang, M.; Shaver, M. P. Polymer-supported Lewis acids and bases: Synthesis and applications. *Prog. Polym. Sci.* **2020**, *111*, 101313.
(22) Mellerup, S. K.; Wang, S. Boron-based stimuli responsive materials. *Chem. Soc. Rev.* **2019**, *48*, 3537−3549.
(23) Ketkov, S.; Rychagova, E.; Kather, R.; Beckmann, J. Pnictogen effects on the electronic interactions in the Lewis pair complexes Ph3EB(C6F5)3 (E = P, As, Sb). *J. Organomet. Chem.* **2021**, *949*, 121944.
(24) Haaland, A. Covalent versus Dative Bonds to Main Group Metals, a Useful Distinction. *Angew. Chem., Int. Ed. Engl.* **1989**, *28*, 992−1007.
(25) Stephan, D. W.; Erker, G. Frustrated Lewis Pairs: Metal-free Hydrogen Activation and More. *Angew. Chem., Int. Ed.* **2010**, *49*, 46−76.
(26) Wang, M.; Nudelman, F.; Matthes, R. R.; Shaver, M. P. Frustrated Lewis Pair Polymers as Responsive Self-Healing Gels. *J. Am. Chem. Soc.* **2017**, *139*, 14232−14236.
(27) Chen, L.; Liu, R.; Yan, Q. Polymer Meets Frustrated Lewis Pair: Second-Generation CO2-Responsive Nanosystem for Sustainable CO2 Conversion. *Angew. Chem., Int. Ed.* **2018**, *57*, 9336−9340.
(28) Schultz, A. R.; Fahs, G. B.; Jangu, C.; Chen, M.; Moore, R. B.; Long, T. E. Phosphonium-containing diblock copolymers from living anionic polymerization of 4-diphenylphosphino styrene. *Chem. Commun.* **2016**, *52*, 950−953.
(29) Fetters, L. J.; Lohse, D. J.; Richter, D.; Witten, T. A.; Zirkel, A. Connection between Polymer Molecular Weight, Density, Chain Dimensions, and Melt Viscoelastic Properties. *Macromolecules* **1994**, *27*, 4639−4647.
(30) Lee, G. Y.; Hu, E.; Rheingold, A. L.; Houk, K. N.; Sletten, E. M. Arene-Perfluoroarene Interactions in Solution. *J. Org. Chem.* **2021**, *86*, 8425−8436.
(31) Dehghan, A.; Shi, A.-C. Modeling Hydrogen Bonding in Diblock Copolymer/Homopolymer Blends. *Macromolecules* **2013**, *46*, 5796−5805.
(32) Tang, C.; Lennon, E. M.; Fredrickson, G. H.; Kramer, E. J.; Hawker, C. J. Evolution of Block Copolymer Lithography to Highly Ordered Square Arrays. *Science* **2008**, *322*, 429−432.
(33) Chao, H.; Koski, J.; Riggleman, R. A. Solvent vapor annealing in block copolymer nanocomposite films: a dynamic mean field approach. *Soft Matter* **2017**, *13*, 239−249.
(34) Massey, A. G.; Park, A. J. Perfluorophenyl derivatives of the elements: I. Tris(pentafluorophenyl)boron. *J. Organomet. Chem.* **1964**, *2*, 245−250.
(35) Jacobsen, H.; Berke, H.; Döring, S.; Kehr, G.; Erker, G.; Fröhlich, R.; Meyer, O. Lewis Acid Properties of Tris-(pentafluorophenyl)borane. Structure and Bonding in L−B(C6F5)3 Complexes. *Organometallics* **1999**, *18*, 1724−1735.
(36) Fielding, L. NMR Methods for the Determination of Protein-Ligand Dissociation Constants. *Curr. Top. Med. Chem.* **2003**, *3*, 39−53.
(37) Rocchigiani, L.; Ciancaleoni, G.; Zuccaccia, C.; Macchioni, A. Probing the Association of Frustrated Phosphine−Borane Lewis Pairs in Solution by NMR Spectroscopy. *J. Am. Chem. Soc.* **2014**, *136*, 112−115.
(38) Beringhelli, T.; Maggioni, D.; D'Alfonso, G. 1H and 19F NMR Investigation of the Reaction of B(C6F5)3 with Water in Toluene Solution. *Organometallics* **2001**, *20*, 4927−4938.
(39) Mai, Y.; Eisenberg, A. Self-assembly of block copolymers. *Chem. Soc. Rev.* **2012**, *41*, 5969−5985.

https://doi.org/10.1021/acspolymersau.1c00024
ACS Polym. Au 2022, 2, 35−41